Soft Landing and Disturbance Rejection for Pneumatic Drives with Partial Position Information

authored by **A. Pfeffer, T. Glück, and A. Kugi**

and published in *Proceedings of the 7th IFAC Symposium on Mechatronic Systems & 15th Mechatronics Forum International Conference.*

Cite this article as:

A. Pfeffer, T. Glück, and A. Kugi, "Soft landing and disturbance rejection for pneumatic drives with partial position information", in *Proceedings of the 7th IFAC Symposium on Mechatronic Systems & 15th Mechatronics Forum International Conference*, vol. 49, Loughborough, UK, Sep. 2016, pp. 559–566. DOI: 10.1016/j.ifacol.2016.10.661

BibTex entry:

```
% This file was created with JabRef 2.9.2.
% Encoding: Cp1252

@INPROCEEDINGS{acinpaper,
  author = {Pfeffer, A. and Gl\"uck, T. and Kugi, A.},
  title = {Soft Landing and Disturbance Rejection for Pneumatic Drives with
       Partial Position Information},
  booktitle = {Proceedings of the 7th IFAC Symposium on Mechatronic Systems \& 15th
       Mechatronics Forum International Conference},
  year = {2016},
  volume = {49},
  number = {21},
  pages = {559-566},
  address = {Loughborough, UK},
  month = {September},
  doi = {10.1016/j.ifacol.2016.10.661}
}
```

Automation and Control Institute (ACIN)
Vienna University of Technology
Gusshausstrasse 27-29/E376
1040 Vienna, Austria

Internet: www.acin.tuwien.ac.at
E-mail: office@acin.tuwien.ac.at
Phone: +43 1 58801 37601
Fax: +43 1 58801 37699

Soft Landing and Disturbance Rejection for Pneumatic Drives with Partial Position Information ⋆

Andreas Pfeffer * **Tobias Glück** * **Andreas Kugi** *

* *Automation and Control Institute, TU Wien, Vienna, Austria (e-mail: {pfeffer,glueck,kugi}@acin.tuwien.ac.at)*

Abstract: Pneumatic drives are used in a wide range of industrial applications. Most of the pneumatic drive applications are simple point-to-point movements, where the motion characteristics is typically set up once by manual tuning. Changes in the operating conditions demand a new manual adjustment and thus additional costs. This work aims at developing a conrol strategy for pneumatic drives to save manual tuning effort and to minimuze the overall system costs. For this cheap position sensors that operate only near the end stops in combination with energy efficient switching valves are used to ensure a smooth movement of the drive and soft landing at the end stops. To pass through the region with no position information, a two-degrees-of-freedom control strategy is employed to account for model uncertainties and disturbances. Inside the position measurement region, compliance control ensures soft landing. The presented strategy is validated by a series of measurements on an experimental test bench.

Keywords: Pneumatic systems; disturbance rejection; impedance control; feedforward control.

1. INTRODUCTION

Pneumatic drives are often used in manufacturing industry, see, e.g., Saidur et al. (2010); Doll et al. (2011). The low investment costs and the high achievable power density makes pneumatic drives particularly suitable for simple handling tasks such as point-to-point movements, see, e.g., Shen et al. (2006); Hildebrandt et al. (2010). There are basically two approaches to perform an point-to-point movement with a pneumatic drive. On the one hand, a servo-pneumatic controller can be used. This approach requires a rather expensive position measuring system but allows to perform a smooth transition of the end-effector, see, e.g., Ilchmann et al. (2006); Richer and Hurmuzlu (2000); Hodgson et al. (2012, 2015). Most of the concepts presented in literature require continuous position sensors over the full stroke length to ensure a high control performance. On the other hand, a simple control strategy may be used, which empties one chamber and fills the other one. This simple switching strategy requires an additional end-of-stroke damper to absorb the resulting high impact energy at the end stops or throttle valves to limit the piston velocity. In the latter approach, the adjustment of the end-of-stroke dampers or the throttle valves turns out to be problematic. Typically, the characteristics of the end-of-stroke damper, i.e., the throttle valve cross sections, have to be manually tuned depending on the supply pressure level and the moving mass. Hence, if the working conditions of a pneumatic drive in a production line change, the damping element or the throttle have to be readjusted, which might require pausing the production. In large pneumatic systems, the supply pressure level varies depending on the distance to the next service unit. This can also lead to the necessity of a costly readjustment of the dampers or the throttle valves. Another common problem in industrial applications are supply pressure drops, which result from several pneumatic loads using the same pressure supply. These pressure drops can lead to lower velocities of the pneumatic piston due to the manually adjusted throttle valves. In this case, the movement may no longer fulfil the timing requirements of the production line.

To overcome these drawbacks, a control strategy is proposed that mimics an end-of-stroke damper. The idea is to place short position sensors close to the desired end positions and to use compliance control to emulate a mass-spring-damper behaviour at the end stops. In order to pass through the range with no position information, a combined position feedforward and pressure feedback control strategy is used.

The actuation of pneumatic drives is classically performed with a costly 5-port/3-way proportional valve, see, e.g., Hildebrandt et al. (2010); Riachy and Ghanes (2014); Toedtheide et al. (2016). In this approach, since only a single input is available, the end-effector position can be controlled but the chamber pressures cannot be influenced separately. Furthermore, due to the construction of proportional valves, they exhibit leakage flows, which reduce the overall energy efficiency, see, e.g., Krichel et al. (2012); Doll et al. (2011). The usage of two pneumatic half-bridges equipped with two cheap 2-port/2-way switching valves each allows to control the end-effector position and the sum pressure of the pneumatic drive. Moreover, it allows to minimize the leakage flows and to ensure cost savings, see, e.g., Saidur et al. (2010); Murrenhoff (2006); Belforte et al. (2004); Ye et al. (1992); van Varseveld and Bone (1997); Schindele et al. (2012); Shen et al. (2006). Hence, this approach is also adopted in this work.

⋆ The authors thank Festo AG & Co. KG for funding this project.

Post-print version of the article: A. Pfeffer, T. Glück, and A. Kugi, "Soft landing and disturbance rejection for pneumatic drives with partial position information", in *Proceedings of the 7th IFAC Symposium on Mechatronic Systems & 15th Mechatronics Forum International Conference*, vol. 49, Loughborough, UK, Sep. 2016, pp. 559–566. doi: 10.1016/j.ifacol.2016.10.661
The content of this post-print version is identical to the published paper but without the publisher's final layout or copy editing.

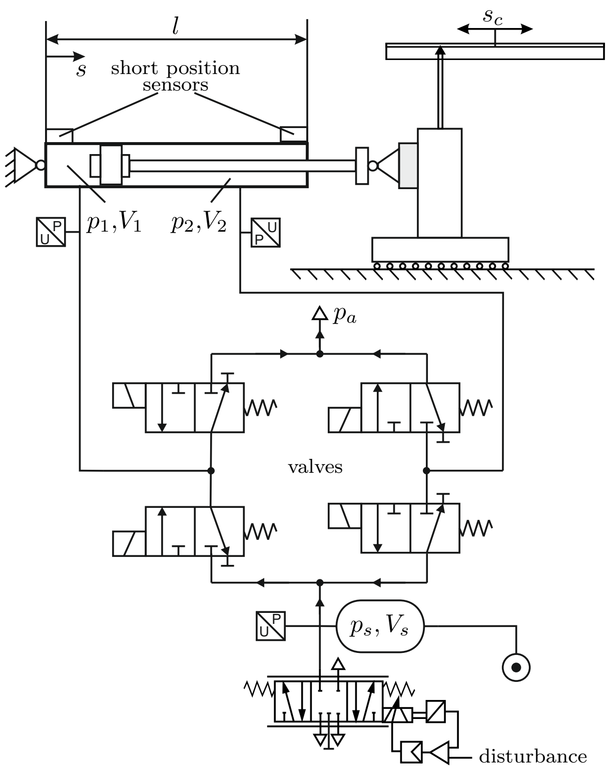

Fig. 1. Schematic of the pneumatic linear drive containing the four fast switching valves, the position sensors, and the proportional valve to realize supply pressure drops.

The paper is organized as follows: Section 2 describes the experimental setup. In Section 3, a mathematical model of the system at hand is presented. Section 4 is devoted to the controller design and Section 5 gives measurement results from the implementation of the proposed control strategy on a test bench. Some conclusions are drawn in Section 6.

2. EXPERIMENTAL SETUP

Fig. 1 shows a schematic of the system under consideration, which consists of a differential cylinder equipped with two short position sensors mounted at the stroke ends with a measurement range of about 50 mm. Low cost pressure sensors are located at the piston inlets and the outlet of the supply pressure chamber. An additional position measuring system provides full position information over the entire stroke to validate the proposed approach. Four fast switching valves, arranged in a full-bridge, control the motion of the piston and the sum pressure. To verify the robustness of the presented control strategy, an additional proportional valve is installed to simulate disturbances in the supply pressure.

3. MATHEMATICAL MODEL

The pneumatic drive can be described by the following set of differential equations, see, e.g., Andersen (2001),

$$\ddot{s} = \frac{1}{m}\left(F_f(\dot{s}) + F_p(p_1,p_2) + F_a\right) \tag{1a}$$

$$\dot{p}_i = \frac{\kappa}{V_i(s)}\left((-1)^i A_i \dot{s} p_i + R\theta_g \dot{m}_i\right),\ i \in \{1,2\}, \tag{1b}$$

with piston position s and chamber pressures p_1 and p_2. In (1a), m denotes the overall moving mass of the system, $F_p(p_1,p_2) = p_1 A_1 - p_2 A_2$ is the pressure force with effective piston areas A_1 and A_2, and $F_a = p_a(A_2 - A_1)$ is the pressure force offset due to the (constant) ambient pressure p_a. Moreover, viscous and Coulomb friction is assumed and modelled by $F_f(\dot{s}) = -c\tanh(\dot{s}/\varepsilon) - d\dot{s}$ with coefficients $\varepsilon \ll 1$, $c > 0$, and $d > 0$. The differential equations for the chamber pressures (1b) contain the chamber volumes $V_1(s) = A_1 s + V_{1,0}$ and $V_2(s) = A_2(l-s) + V_{2,0}$, with dead volumes $V_{1,0}$ and $V_{2,0}$ and maximal stroke length l, the specific gas constant R, the (constant) gas temperature θ_g, and the specific heat ratio κ. Since the valve dynamics are reasonably fast compared to the temperature and pressure dynamics, the instantaneous switching of the valves is assumed in the following. Furthermore, assuming an adiabatic lossless flow, the mass flows $\dot{m}_i$ can be described, according to ISO 6358 (2012), by

$$\dot{m}_1 = C_{1s}\Gamma_{1s}(p_1) - C_{a1}\Gamma_{a1}(p_1) \tag{2a}$$

$$\dot{m}_2 = C_{2s}\Gamma_{2s}(p_2) - C_{a2}\Gamma_{a2}(p_2), \tag{2b}$$

with pneumatic conductances $C_{ij} = \{0, C_{\max}\}$ and

$$\Gamma_{ij}(p_i) = \rho_0 p_j \Psi\left(p_i/p_j\right)\ , \tag{3}$$

where $\rho_0 = 1.1845\,\mathrm{kg/m^3}$ denotes the technical density and p_s is the supply pressure. In (3),

$$\Psi\left(\Pi_{ij}\right) = \begin{cases} \sqrt{1 - \left(\frac{\Pi_{ij}-\Pi_c}{1-\Pi_c}\right)^2} & \text{for} \quad \Pi_{ij} \geq \Pi_c \\ 1 & \text{for} \quad \Pi_{ij} < \Pi_c \end{cases} \tag{4}$$

represents the flow-through function with pressure ratios $\Pi_{ij} = p_i/p_j$ and critical pressure ratio $\Pi_c \geq 0$. In the application at hand, the conductances C_{ij} are pulse-width modulated (pwm). For $k = 0,1,\ldots$ they read as

$$C_{ij} = \begin{cases} C_{\max} & \text{for} \quad \left(k + \frac{1-\chi_{ij}}{2}\right)T < t \leq \left(k + \frac{1+\chi_{ij}}{2}\right)T \\ 0 & \text{else}\ , \end{cases} \tag{5}$$

where $\chi_{ij} \in [0,1]$ are the duty ratios and T is the fixed modulation period. The pulse-width modulation results in modulated state variables. In the following, an average model is derived from (1). For this, the mean value $\bar{\xi}$ of a variable ξ over a modulation period T is introduced in the form

$$\bar{\xi} = \frac{1}{T}\int_{t-T}^{t} \xi(\tau)\,\mathrm{d}\tau. \tag{6}$$

Because the modulation period T can be chosen sufficiently small, only small variations $\Delta\xi$ of the variables ξ are considered within a modulation period, i.e., $\xi = \bar{\xi} + \mathcal{O}(\Delta\xi)$ with Landau symbol $\mathcal{O}(\cdot)$. Moreover, for small position and pressure variations, the functions $\Gamma_{ij}(p_i)$ according to (3) and the chamber volumes $V_i(s)$ may be written as $\Gamma_{ij}(p_i) = \Gamma_{ij}(\bar{p}_i) + \mathcal{O}(\Delta p_i)$ and $V_i(s) = V(\bar{s}) + \mathcal{O}(\Delta s)$. This allows us to infer an average model from (1) in the form

$$\ddot{\bar{s}} = \frac{1}{m}\left(F_f(\dot{\bar{s}}) + F_p(\bar{p}_1,\bar{p}_2) + F_a\right) \tag{7a}$$

$$\dot{\bar{p}}_i = \frac{\kappa}{V_i(\bar{s})}\left((-1)^i A_i \dot{\bar{s}} \bar{p}_i + R\theta_g \dot{\bar{m}}_i\right),\ i \in \{1,2\}, \tag{7b}$$

Post-print version of the article: A. Pfeffer, T. Glück, and A. Kugi, "Soft landing and disturbance rejection for pneumatic drives with partial position information", in *Proceedings of the 7th IFAC Symposium on Mechatronic Systems & 15th Mechatronics Forum International Conference*, vol. 49, Loughborough, UK, Sep. 2016, pp. 559–566. DOI: 10.1016/j.ifacol.2016.10.661
The content of this post-print version is identical to the published paper but without the publisher's final layout or copy editing.

with

$$\dot{\bar{m}}_1 = C_{\max}\big(\Gamma_{1s}(\bar{p}_1)\chi_{1s} - \Gamma_{a1}(\bar{p}_1)\chi_{a1}\big) \tag{7c}$$

$$\dot{\bar{m}}_2 = C_{\max}\big(\Gamma_{2s}(\bar{p}_2)\chi_{2s} - \Gamma_{a2}(\bar{p}_2)\chi_{a2}\big) \tag{7d}$$

and inputs $\chi_{ij} \in [0,1]$, $ij \in \{1s,a1,2s,a2\}$.

4. CONTROLLER DESIGN

Basically, the goal is to perform a point-to-point movement of the piston from one end stop to the other. To move the piston trough the region without position information, two independent pressure controllers are used. Close to the end stops, where the piston position can be measured, a compliance controller mimics the behaviour of a mass-spring-damper system to ensure soft landing at the end stops. A sequence control strategy is proposed to perform a closed extension and retraction cycle of the piston rod with a given cycle time.

4.1 Pressure Control

As discussed in the introduction, position control cannot be realized over the whole piston stroke because the position information is only available near the end stops. By contrast, the pressures $\bar{p}_1$ and $\bar{p}_2$ are measured during the whole movement. Thus, pressure control is used to account for model inaccuracies in the pneumatic subsystem, e.g., uncertainties in the conductances, dead volumes, etc. Feedback linearization, see Isidori (1995), applied to (7b) with outputs $y_i = \bar{p}_i$ for $i \in \{1,2\}$ yields

$$\dot{\bar{m}}_i = \frac{1}{g_i}\left(\alpha_i - f_i\right)\ ,\ i \in \{1,2\}, \tag{8a}$$

with

$$f_i = \frac{\kappa}{V_i(\bar{s})}(-1)^i A_i \dot{\bar{s}}\bar{p}_i\ , \quad g_i = \frac{\kappa R \theta_g}{V_i(\bar{s})}\ . \tag{8b}$$

The control inputs are given by

$$\chi_{is} = \begin{cases} \frac{\dot{\bar{m}}_i}{C_{\max}\Gamma_{is}(\bar{p}_i)}\ , & \dot{\bar{m}}_i \geq 0 \\ 0\ , & \dot{\bar{m}}_i < 0 \end{cases} \tag{8c}$$

$$\chi_{ai} = \begin{cases} 0\ , & \dot{\bar{m}}_i \geq 0 \\ -\frac{\dot{\bar{m}}_i}{C_{\max}\Gamma_{ai}(\bar{p}_i)}\ , & \dot{\bar{m}}_i < 0\ . \end{cases} \tag{8d}$$

The new control inputs α_i in (8a) read as

$$\alpha_i = \dot{\bar{p}}_i^d - a_{i,0}e_i - a_{i,1}\int_0^t e_i\, \mathrm{d}\tau\ , \tag{8e}$$

with the pressure references $\bar{p}_i^d$, the pressure errors $e_i = \bar{p}_i - \bar{p}_i^d$, and the constant controller parameters $a_{i,j} > 0$, $j = 0,1$, $i \in \{1,2\}$. Application of (8) to (7b) allows to assign a linear and exponentially stable error dynamics.

4.2 Trajectory Planning

To realize a pressure control concept, sufficiently smooth reference trajectories $\bar{p}_i^d$ have to be planned. Since the system (7) is differentially flat with flat outputs $w_1 = \bar{s}$ and $w_2 = \bar{p}_1 + \bar{p}_2$, see, e.g., Hildebrandt et al. (2010), it is possible to parametrize all states in terms of the desired flat outputs w_1^d and w_2^d and their time derivatives

$$\bar{s}^d = w_1^d \tag{9a}$$

$$\dot{\bar{s}}^d = \dot{w}_1^d \tag{9b}$$

$$\bar{p}_1^d = \psi_1\big(w_2^d,\dot{w}_1^d,\ddot{w}_1^d\big) = -\frac{1}{A_1+A_2}\big(-m\ddot{w}_1^d + F_f\big(\dot{w}_1^d\big) - A_2 w_2^d + F_a\big) \tag{9c}$$

$$\bar{p}_2^d = \psi_2\big(w_2^d,\dot{w}_1^d,\ddot{w}_1^d\big) = w_2^d + \frac{1}{A_1+A_2}\big(-m\ddot{w}_1^d + F_f\big(\dot{w}_1^d\big) - A_2 w_2^d + F_a\big)\ . \tag{9d}$$

The relative degrees of w_1 and w_2 with respect to the inputs $\dot{\bar{m}}_1$ and $\dot{\bar{m}}_2$ reads as $r_1 = 3$ and $r_2 = 1$. Thus, polynomial reference trajectories of class $\mathcal{C}^{r_1}$

$$w_1^d(t) = w_1^d(t_0) + \big(w_1^d(t_f) - w_1^d(t_0)\big)\sum_{j=r_1+1}^{2r_1+1} b_{1j}\left(\frac{t}{t_f}\right)^j\ , \tag{10}$$

and of class $\mathcal{C}^{r_2}$

$$w_2^d(t) = \begin{cases} \underline{w}_2^d(t)\ , & t_0 \leq t \leq t_1 \\ \overline{w}_2^d(t)\ , & t_1 < t \leq t_f\ , \end{cases} \tag{11}$$

with

$$\underline{w}_2^d(t) = w_2^d(t_0) + \big(w_2^d(t_1) - w_2^d(t_0)\big)\sum_{j=r_2+1}^{2r_2+1} b_{2j}\left(\frac{t}{t_1}\right)^j\ ,$$

$$\overline{w}_2^d(t) = w_2^d(t_1) + \big(w_2^d(t_2) - w_2^d(t_1)\big)\sum_{j=r_2+1}^{2r_2+1} b_{2j}\left(\frac{t-t_1}{t_2}\right)^j\ ,$$

starting time t_0, intermediate time t_1, end time t_f, and $t_2 = t_f - t_1$ are chosen. The coefficients b_{ij} are given in closed form by

$$b_{ij} = \frac{(-1)^{j-r_i-1}(2r_i+1)!}{j r_i!(j-r_i-1)!(2r_i+1-j)!}\ ,\ i \in \{1,2\}\ , \tag{12}$$

see Piazzi and Visioli (2001). The reference $w_2^d(t)$ is split up into two time intervals to obtain an easily parametrizable feasible reference with short transition time $t_f - t_0$. To make this clear, Fig. 2 exemplarily depicts two reference trajectories with starting time $t_0 = 0\,\mathrm{s}$, end time $t_f = 0.7\,\mathrm{s}$, initial values $w_1^d(t_0) = 0\,\mathrm{m}$ and $w_2^d(t_0) = 2.5\,\mathrm{bar}$, end values $w_1^d(t_f) = 0.4\,\mathrm{m}$ and $w_2^d(t_f) = 2.5\,\mathrm{bar}$, and intermediate value $w_2^d(t_1) = 6\,\mathrm{bar}$. The trajectories only differ in the intermediate time t_1. In Fig. 2, on the left, the intermediate time is set to $t_1 = 0.44\,\mathrm{s}$. The control input χ_{a2} nearly hits the upper constraint at $t \approx 0.07\,\mathrm{s}$. In Fig. 2, on the right, the intermediate time is shifted to $t_1 = 0.35\,\mathrm{s}$, which brings along a balancing of the control effort.

4.3 Compliance Control

As described before, the position is only measured close to the stroke ends and the reference trajectory w_1^d ends within this region. The distance of the measurement region is passed through using a compliance control strategy. The fundamental idea of compliance control is to design a controller which imposes a certain reference dynamics, e.g., in the form of a desired mass-spring-damper system

$$m\ddot{\bar{s}} = F^r\big(\bar{s},\dot{\bar{s}},\bar{s}^r\big) = -d^r\dot{\bar{s}} - c^r(\bar{s} - \bar{s}^r), \tag{13}$$

with spring constant c^r, damping constant d^r, and constant reference position $\bar{s}^r$. Note that without a force sensor, no mass shaping can be realized, see, e.g., Ott et al. (2008).

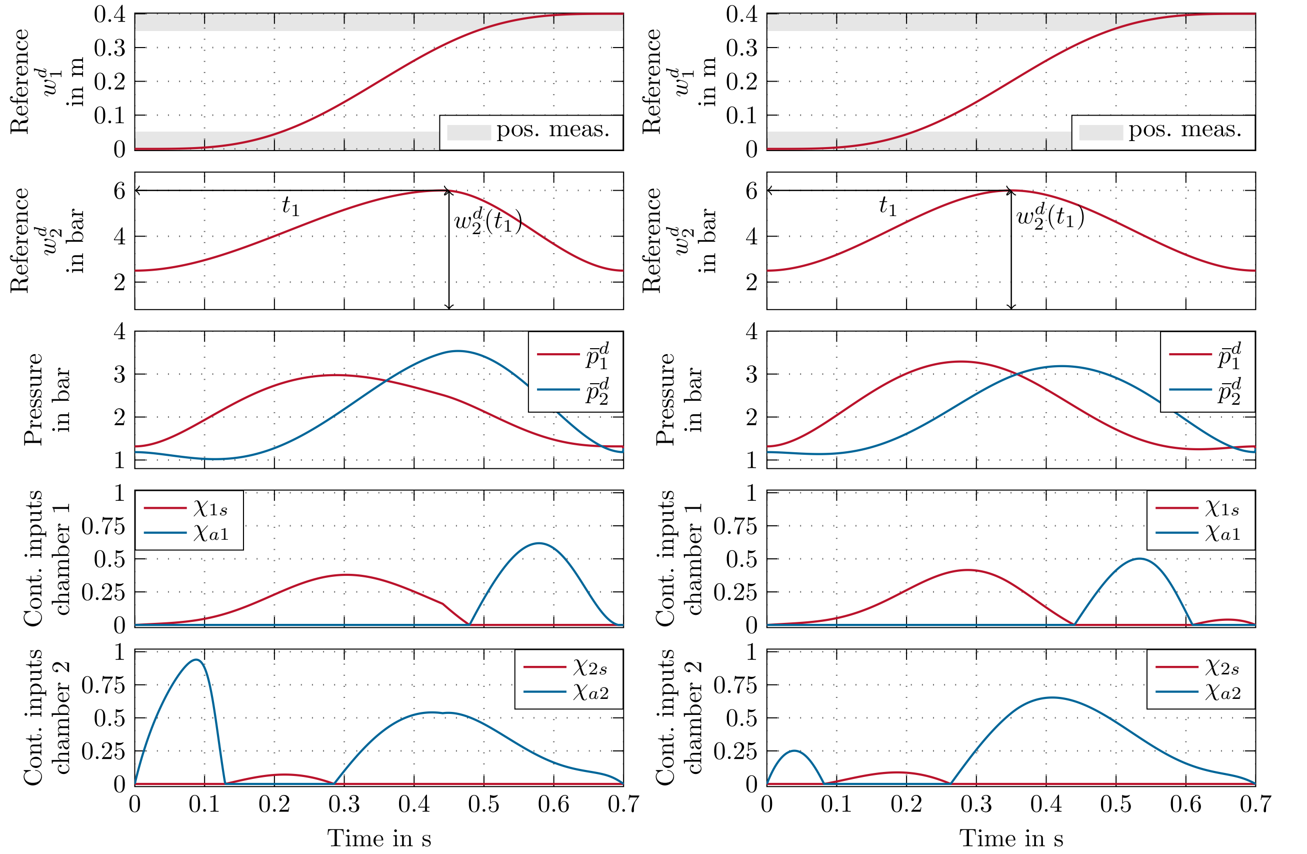

Fig. 2. Reference trajectories, chamber pressures and control inputs for the extension (left) and retraction (right) of the piston.

Combining (7a) and (13) with the new input $v = F_p(\bar{p}_1, \bar{p}_2)$ results in

$$v = F^r(\bar{s}, \dot{\bar{s}}, \bar{s}^r) - F_f(\dot{\bar{s}}) - F_a \ . \tag{14a}$$

The pneumatic full-bridge allows to separately control both chamber pressures $\bar{p}_1$ and $\bar{p}_2$. These two degrees of freedom are used to impose the reference dynamics (13) and to minimize the sum pressure $\bar{p}_1 + \bar{p}_2$ which in turn minimizes the air consumption. Hence, using the subordinate pressure controller (8), the reference values $\bar{p}_i^d$ are chosen as

$$\bar{p}_1^d = \begin{cases} \frac{p_{2,\min} A_2 + v}{A_1} \ , & v \geq 0 \\ p_{1,\min} \ , & v < 0 \end{cases} \tag{14b}$$

$$\bar{p}_2^d = \begin{cases} p_{2,\min} \ , & v \geq 0 \\ \frac{p_{1,\min} A_1 - v}{A_2} \ , & v < 0 \ , \end{cases} \tag{14c}$$

with constant pressures $p_{1,\min}$ and $p_{2,\min}$. A numerical differentiator is used to approximately calculate the time derivative $\dot{\bar{p}}_i^d$ of the reference $\bar{p}_i^d$. The reference position $\bar{s}^r$ in (14a) is adjusted to get a specific pressure force $\tilde{F}^r$ at the end stops.

4.4 Sequence Control Strategy

In the following, a sequence control strategy for the extension and retraction of the piston rod is introduced. Fig. 3 depicts a flow chart of the sequence control scheme.

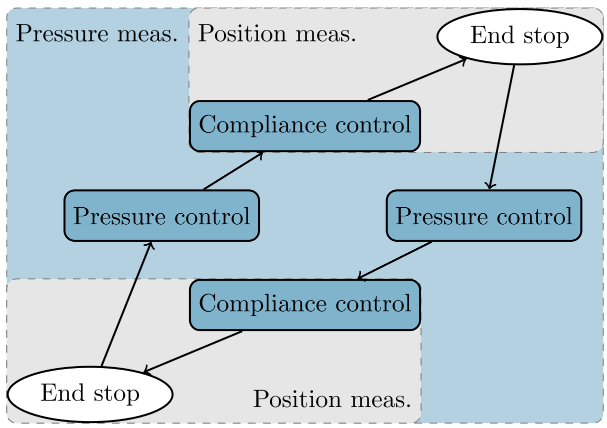

Fig. 3. Flow chart of the sequence control strategy.

The background is coloured blue and grey to indicate where pressure and position information is available. Starting at an end stop, the piston is moved by pressure control according to (8) towards the opposite end stop inside the respective position measurement region. Within this region, compliance control according to (14) is activated, which ensures soft landing at the end stop. If the planned trajectory does not move the piston inside the respective position measurement region because of a disturbance, the

Post-print version of the article: A. Pfeffer, T. Glück, and A. Kugi, "Soft landing and disturbance rejection for pneumatic drives with partial position information", in *Proceedings of the 7th IFAC Symposium on Mechatronic Systems & 15th Mechatronics Forum International Conference*, vol. 49, Loughborough, UK, Sep. 2016, pp. 559–566. DOI: 10.1016/j.ifacol.2016.10.661
The content of this post-print version is identical to the published paper but without the publisher's final layout or copy editing.

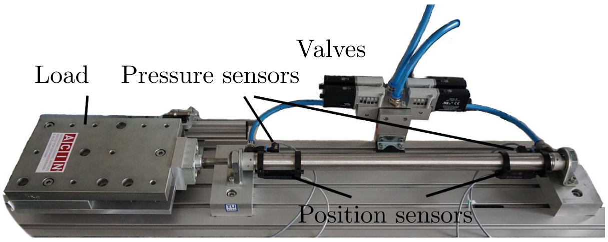

Fig. 4. Picture of the lab test bench.

compliance controller, which is activated on a triggered time base, will help out. Due to the fact that the actual piston position is unknown, the position $\bar{s}$ is set to the last available position measurement. The piston is accelerated by the compliance controller until the piston reaches the measurement region. Then, the position is set to the measured position and the piston is moved towards the end stop.

5. TEST BENCH AND MEASUREMENT RESULTS

In this section, measurements are shown to validate the proposed control strategy. Fig. 4 depicts a picture of the lab test bench. The test bench is equipped with a Festo DNSU-25-400-PPV-A cylinder, four Festo MHA3-MS1H-3/2G-3-K switching valves, two Festo SDAT-MHS-M50-1L-SA-E-0.3-M8 (Hall effect sensor) position sensors, and three Festo SPTE pressure sensors to measure the chamber pressures and the supply pressure.[1] In addition, a high performance MTS Sensor Temposonics® R-series magnetostrictive full stroke position sensor is used to verify the data. Note that the built-in manually adjustable dampers of the cylinder are deactivated.

5.1 Nominal Case

In order to examine the nominal case, a supply pressure buffer of $V_s = 20\,\mathrm{l}$ is used in combination with an industrial standard Festo MS6 series service unit which includes a mechanical pressure controller. Fig. 5 shows the extension and retraction of the piston rod for this nominal case. On top, the supply pressure is shown. The oscillations in the supply pressure signal result from the pwm-controlled valves. The gray background refers to the timespan where the piston reaches the position measurement region and the compliance controller is activated. As can be seen, the position matches the reference quite well, which indicates that the mathematical model from Section 3 is an accurate approximation of the real system. In the first 0.5 s, the pressure measurements and the control inputs show high frequency oscillations due to the pwm-controlled valves. The deviation in $\bar{p}_1$ for the extension and in $\bar{p}_2$ for the retraction movement at 0.1 s predominantly result from the rather small control inputs χ_{2s} and χ_{1s}, respectively. Because of the limited switching valve dynamics the stipulation of the instantaneous opening and closing of the switching valves is violated for small control inputs.

[1] The total costs of all sensors required for the presented approach are less than the price of a typical full-stroke position sensor, in particular for large cylinder strokes.

5.2 Model Uncertainties

In this section, a scenario is investigated, which exhibits the benefits of additional pressure control during the movement of the rod to counteract model uncertainties. In the following, model uncertainties are emulated by enlarging the pipe lengths between the valves and the cylinder from 30 cm in the nominal case up to a factor of five to 150 cm. This brings along a significant increase of the chamber dead volumes and the time delays. In Fig. 6, the signals are indexed with the corresponding pipe lengths. On the left, the movement with pure feedforward control in the position sensorless region is shown. To make this clear, the input χ_{1s} is shown exemplarily. The longer the pipes, the higher the velocity during the movement. As a result, the piston hits the end stop at $t \approx 0.55\,\mathrm{s}$, which can be seen in rapid changes in the velocity. In contrast to this, the additional pressure feedback control, shown on the right in Fig. 6, ensures lower variations in the velocity during the movement. Hence a soft landing can be realized.

5.3 Varying Supply Pressure and Supply Pressure Drops

As already mentioned in the introduction, different supply pressure levels and supply pressure drops are a common problem in industrial applications. To mimic this behaviour, a Festo MPYE-5-1/8-HF-010 B proportional valve is used to control the supply pressure level for this experiment. In addition, to achieve significant pressure drops during the movement, the supply pressure buffer is reduced to $V_s = 0.75\,\mathrm{l}$. Furthermore, an additional Festo MPYE-5-3/8-010 B proportional valve, which allows high volume flows due to its large cross section, is installed to deflate the supply pressure buffer during the movement. Fig. 7 shows the position measurement and the supply pressure p_s for a couple of extension and retraction cycles of the piston rod. The supply pressure is varied after two cycles. The first cycle is without and the second one with activated disturbance. Therefore, the deflate valve is fully opened. The supply pressure is varied from $p_s = 8\,\mathrm{bar}$ to approximately $p_s = 3.5\,\mathrm{bar}$. As can be seen in Fig. 7, even with the disturbance, the desired movement can be realized until a critical supply pressure level is reached. This happens at $t \approx 75\,\mathrm{s}$, see the zoom-in part, where the supply pressure is too low for the reference trajectory. However, the compliance control strategy is able to handle this fault and moves the piston to the end stop.

A more detailed view is given in Fig. 8. Here, the nominal and the disturbed movement, labeled with *, are shown. The supply pressure is set to $p_s = 8\,\mathrm{bar}$ for the first movement. In the disturbed case, the disturbance proportional valve is opened for 250 ms which results in a supply pressure drop of 1.8 bar. The pressure drops are compensated by the pressure controller and the resulting movement is almost equal to the nominal case.

6. CONCLUSIONS

In this work, a robust soft landing strategy for pneumatic linear drives with position information only near the end stops was presented. To this end, a combined position feedforward and pressure feedback control strategy is proposed. The trajectory planning is based on sufficiently

Post-print version of the article: A. Pfeffer, T. Glück, and A. Kugi, “Soft landing and disturbance rejection for pneumatic drives with partial position information”, in *Proceedings of the 7th IFAC Symposium on Mechatronic Systems & 15th Mechatronics Forum International Conference*, vol. 49, Loughborough, UK, Sep. 2016, pp. 559–566. doi: 10.1016/j.ifacol.2016.10.661
The content of this post-print version is identical to the published paper but without the publisher’s final layout or copy editing.

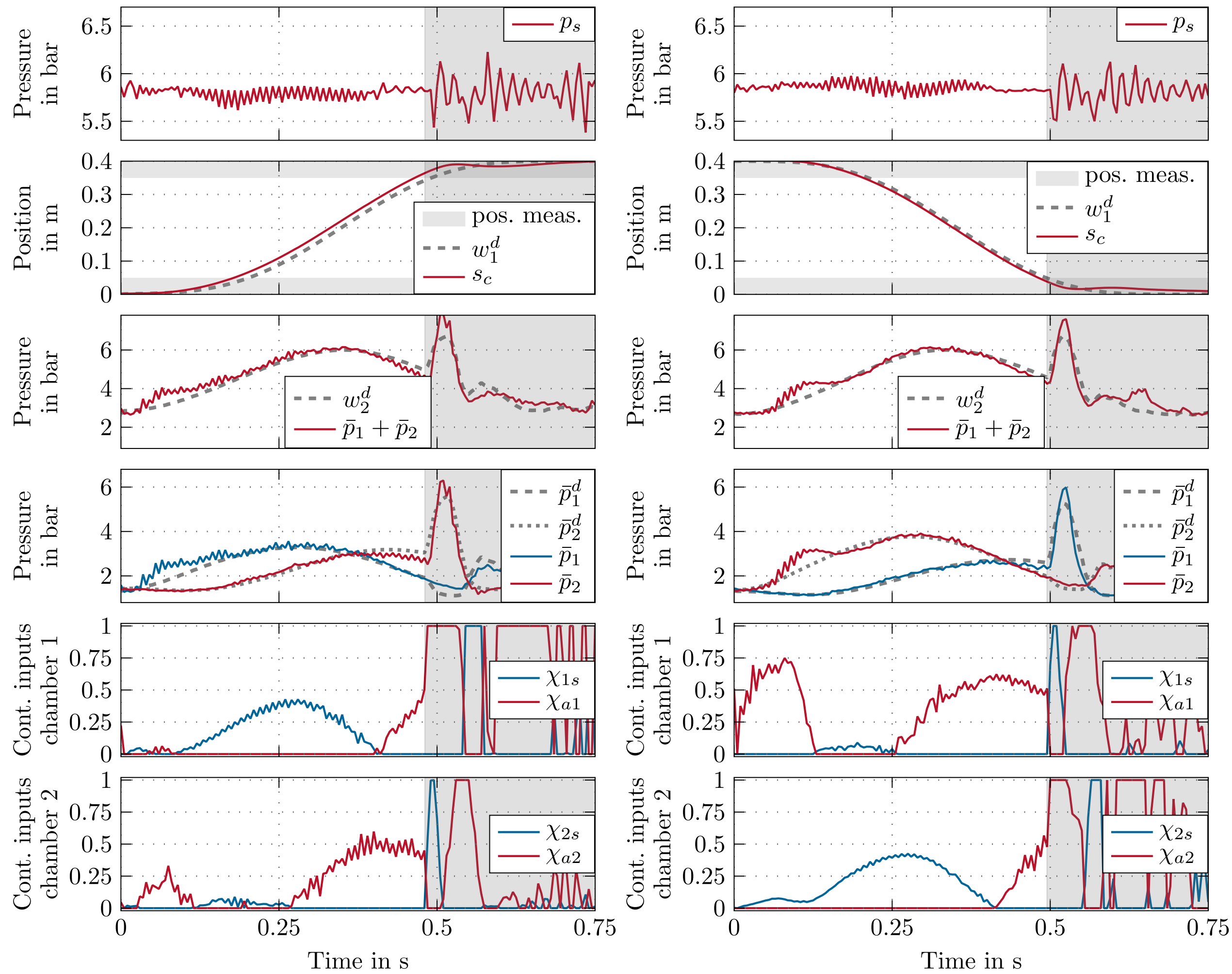

Fig. 5. Measurement results for the extension (left) and retraction (rigth) of the piston for the nominal case with a supply pressure buffer volume of $V_s = 20\,\mathrm{l}$ and an industrial standard service unit with a mechanical pressure controller.

smooth piecewise polynomials. To control the piston in the regions close to the end stops, where position information is available, a compliance control strategy is derived, which emulates a desired mass-spring-damper system. The whole strategy was tested on a test bench with a pneumatic differential cylinder and validated with measurements. The results show that the presented strategy can be used for simple point-to-point movements in various industrial applications like sorting in production lines, in particular also due to its robustness against different supply pressure levels, pressure drops, and varying uncertainties. Hence, costly manual readjustments of throttle valves or mechanical dampers can be saved. Future work will be concerned with additional parameter estimation strategies to iteratively adapt the controller.

REFERENCES

Andersen, B.W. (2001). *The Analysis and Design of Pneumatic Systems*. Krieger Publishing Company.

Belforte, G., Mauro, S., and Mattiazzo, G. (2004). A method for increasing the dynamic performance of pneumatic servosystems with digital valves. *Mechatronics*, 14(11), 1105–1120.

Doll, M., Neumann, R., and Sawodny, O. (2011). Energy efficient use of compressed air in pneumatic drive systems for motion tasks. In *Proc. of the 2011 International Conference on Fluid Power and Mechatronics (FPM)*, 340–345. Beijing, China.

Hildebrandt, A., Neumann, R., and Sawodny, O. (2010). Optimal system design of siso-servopneumatic positioning drives. *IEEE Transactions on Control Systems Technology*, 18(1), 35–44.

Hodgson, S., Tavakoli, M., Pham, M., and Leleve, A. (2015). Nonlinear discontinuous dynamics averaging and PWM-based sliding control of solenoid-valve pneumatic actuators. *IEEE/ASME Transactions on Mechatronics*, 20(2), 876–888.

Hodgson, S., Le, M.Q., Tavakoli, M., and Pham, M.T. (2012). Improved tracking and switching performance of an electro-pneumatic positioning system. *Mechatronics*, 22(1), 1–12.

Ilchmann, A., Sawodny, O., and Trenn, S. (2006). Pneumatic cylinders: Modelling and feedback force-control. *International Journal of Control*, 79(6), 650–661.

Isidori, A. (1995). *Nonlinear Control Systems*. Springer, 3rd edition.

Post-print version of the article: A. Pfeffer, T. Glück, and A. Kugi, "Soft landing and disturbance rejection for pneumatic drives with partial position information", in *Proceedings of the 7th IFAC Symposium on Mechatronic Systems & 15th Mechatronics Forum International Conference*, vol. 49, Loughborough, UK, Sep. 2016, pp. 559–566. DOI: 10.1016/j.ifacol.2016.10.661
The content of this post-print version is identical to the published paper but without the publisher's final layout or copy editing.

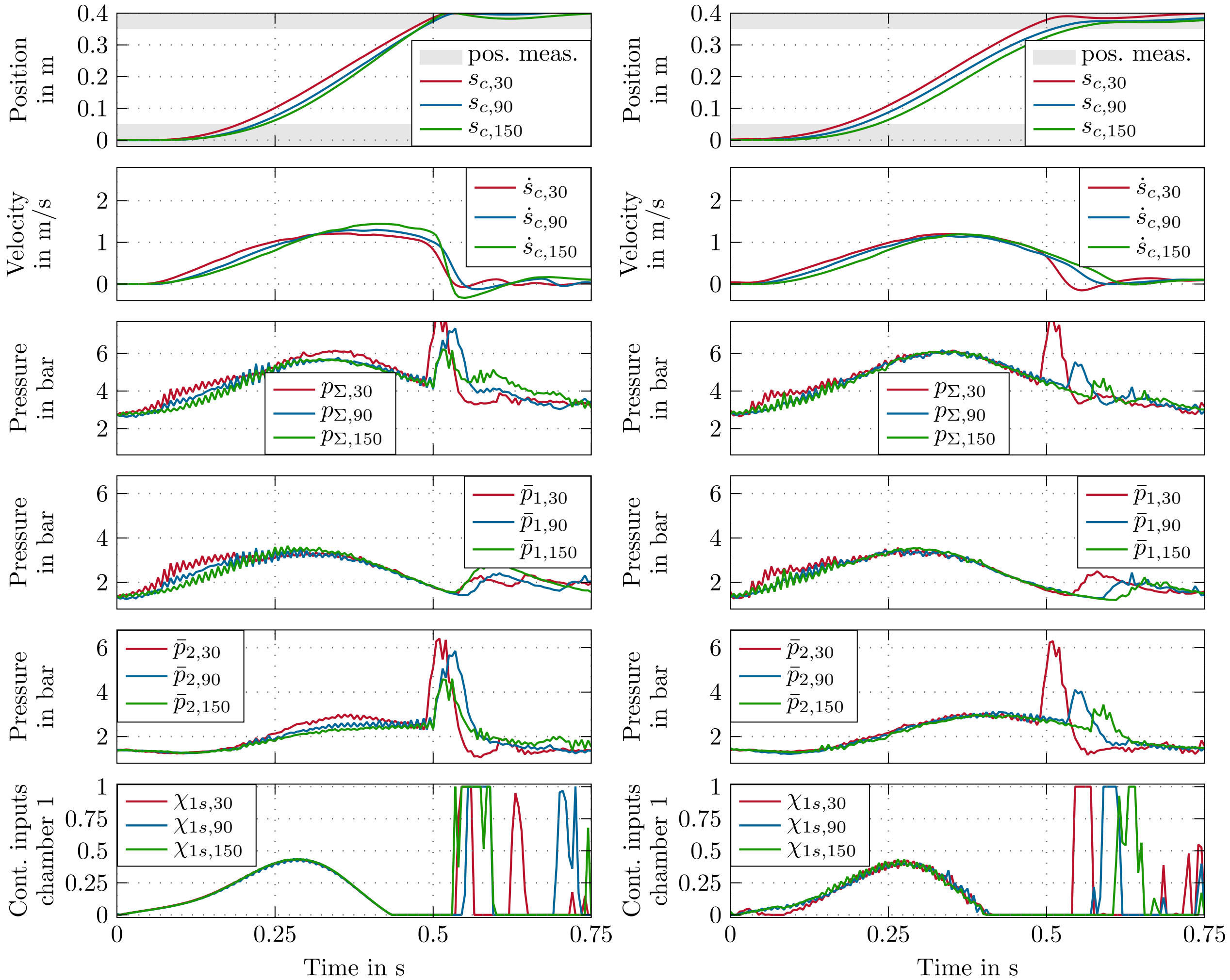

Fig. 6. Measurement results for the extension of the piston rod with feedforward control only on the left and additional feedback pressure control on the right for different pipe lengths.

ISO 6358 (2012). URL `http://www.iso.org`. Access: 08.02.2016.

Krichel, S., Hülsmann, S., Hirzel, S., Elsland, R., and Sawodny, O. (2012). Mehr Klarheit bei der Druckluft. *O+P, Ölhydraukik und Pneumatik*, 1-2, 28–32.

Murrenhoff, H. (2006). *Grundlagen der Fluidtechnik - Teil 2: Pneumatik*. Shaker.

Ott, C., Kugi, A., and Hirzinger, G. (2008). On the passivity-based impedance control of flexible joint robots. *IEEE Transactions on Robotics*, 24(2), 416–429.

Piazzi, A. and Visioli, A. (2001). Optimal noncausal set-point regulation of scalar systems. *Automatica*, 37, 121–127.

Riachy, S. and Ghanes, M. (2014). A nonlinear controller for pneumatic servo systems: Design and experimental tests. *IEEE/ASME Transactions on Mechatronics*, 19(4), 1363–1373.

Richer, E. and Hurmuzlu, Y. (2000). A high performance pneumatic force actuator system: Part ii—nonlinear controller design. *Journal of Dynamic Systems, Measurement, and Control*, 122(3), 426–434.

Saidur, R., Rahim, N., and Hasanuzzaman, M. (2010). A review on compressed-air energy use and energy savings. *Journal of Renewable and Sustainable Energy Reviews*, 14(4), 1135–1153.

Schindele, D., Prabel, R., and Aschemann, H. (2012). Nonlinear model predictive control of an electro-pneumatic clutch for truck applications. In *Proc. of the 7th Vienna Conference on Mathematical Modelling (Mathmod)*, 526–531. Vienna, Austria.

Shen, X., Zhang, J., Barth, E.J., and Goldfarb, M. (2006). Nonlinear model-based control of pulse width modulated pneumatic servo systems. *Journal of Dynamic Systems, Measurement, and Control*, 128(3), 663–669.

Toedtheide, A., Lilge, T., and Haddadin, S. (2016). Antagonistic impedance control for pneumatically actuated robot joints. *IEEE Robotics and Automation Letters*, 1(1), 161–168.

van Varseveld, R. and Bone, G. (1997). Accurate position control of a pneumatic actuator using on/off solenoid valves. *IEEE/ASME Transactions on Mechatronics*, 2(3),

Post-print version of the article: A. Pfeffer, T. Glück, and A. Kugi, "Soft landing and disturbance rejection for pneumatic drives with partial position information", in *Proceedings of the 7th IFAC Symposium on Mechatronic Systems & 15th Mechatronics Forum International Conference*, vol. 49, Loughborough, UK, Sep. 2016, pp. 559–566. DOI: 10.1016/j.ifacol.2016.10.661

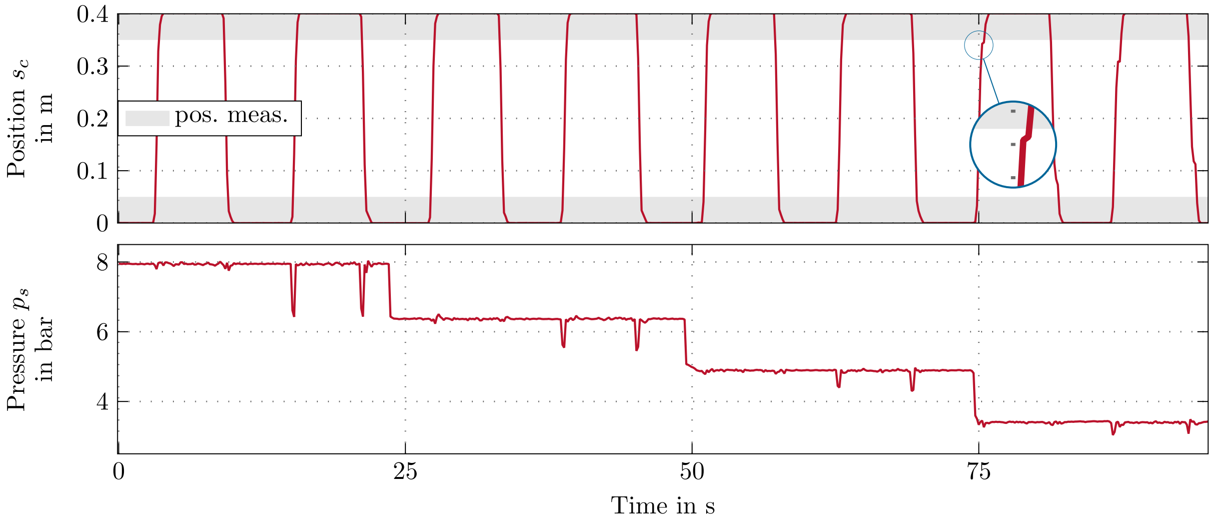

Fig. 7. Measurement results for a varying supply pressure and supply pressure drops during the movement.

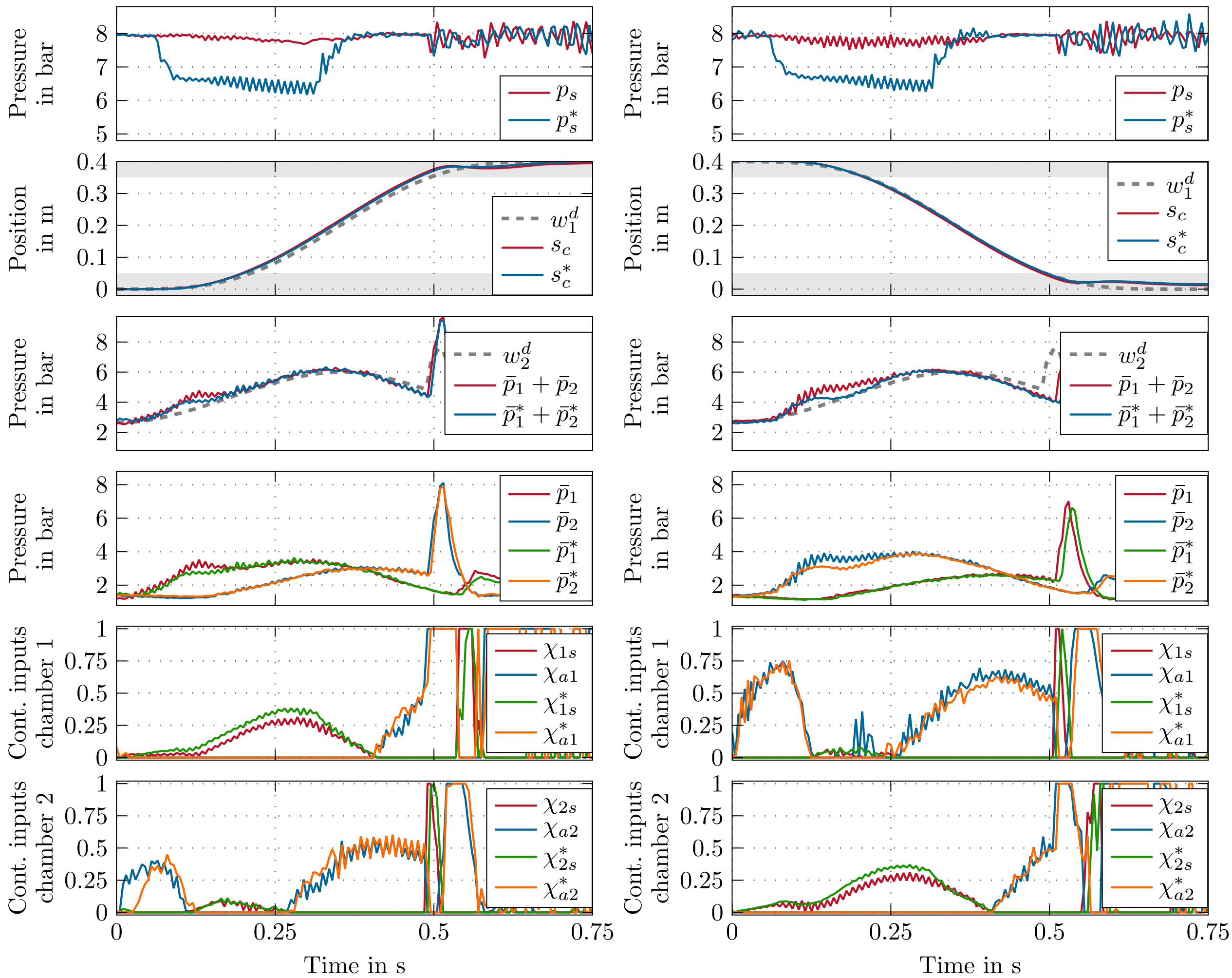

Fig. 8. Measurement results for fast supply pressure drops, for extension (left) and retraction (right) of the piston.

195–204.

Ye, N., Scavarda, S., Betemps, M., and Jutard, A. (1992). Models of a pneumatic PWM solenoid valve for engineering applications. *Journal of Dynamic Systems, Measurement, and Control*, 114(4), 680–688.

Post-print version of the article: A. Pfeffer, T. Glück, and A. Kugi, “Soft landing and disturbance rejection for pneumatic drives with partial position information”, in *Proceedings of the 7th IFAC Symposium on Mechatronic Systems & 15th Mechatronics Forum International Conference*, vol. 49, Loughborough, UK, Sep. 2016, pp. 559–566. DOI: 10.1016/j.ifacol.2016.10.661

The content of this post-print version is identical to the published paper but without the publisher’s final layout or copy editing.